



Selective Detection of Silver Ions Based on Resonance Rayleigh Scattering Spectrometry Using Colloidal Silica Nanoparticles

Justine Dagher¹ · Riham El Kurdi¹ · Digambara Patra¹

Received: 5 January 2022 / Accepted: 22 March 2022 / Published online: 4 April 2022
© The Author(s), under exclusive licence to Springer Science+Business Media, LLC, part of Springer Nature 2022

Abstract

Colloidal silica or silicon dioxide nanoparticles (SiO₂ NPs) are extremely amorphous nanomaterials owing spherical shape. These nanoparticles have gained much interest due to their usage in various fields; going from the industrial domain to the biomedical field. In this study, the synthesis of SiO₂ NPs was investigated and optimized by varying two essential parameters including the type of silica precursor and the concentration of sodium hydroxide. The suitable nanoparticles were formed according to the best silica precursor (Colloidal Silica) and the optimum NaOH concentration (C = 100 mM). The applicability of the prepared nanoparticles was performed for the detection of silver ions in the concentration range between 5 and 300 μM based on resonance Rayleigh scattering (RRS) spectrometry. The limit of detection obtained was equal to 130 nM and the recovery percentage was between 98.4 and 100.4%. The detection of silver ions based on RRS technique was found to be easy to manipulate, simple and fast with low cost, compared to the usual techniques used as chromatography and calorimetric techniques.

Keywords SiO₂ nanoparticles · Optimization · Detection · Ag⁺ · RRS

Introduction

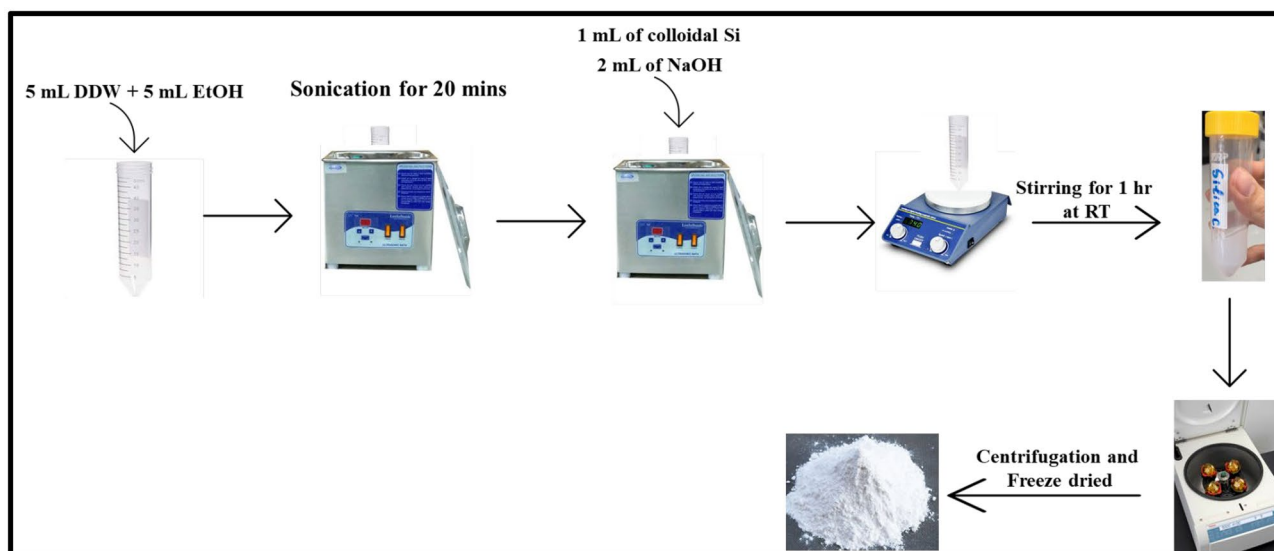
Nanoparticles are defined as particles that have a diameter between 1 and 100 nm [1]. In fact, colloidal silica nanoparticles, also called silicon dioxide (SiO₂ NPs), are amorphous nanoparticles produced in spherical shape. SiO₂ NPs can be synthesized based on several techniques as reverse micro-emulsion, flame synthesis, and sol–gel method [2]. Mainly, silica nanoparticles have unique properties especially high chemical stability, biocompatibility, and targeted controlled release. Generally, the Si–O bond of the silica is responsible for their higher stability [3]. In fact, SiO₂ NPs can be synthesized in different sizes, shapes and different surface area. These properties expand the use of these nanomaterials in different domains [4]. Furthermore, silicon dioxide nanoparticles possess significant benefits such as their high biocompatibility and hydrophobicity, high systemic stability. Additionally, SiO₂ NPs can highly resist to pH changes, and present large multi-functionality, due to their low toxicity [5].

Lately, researchers have developed the use of nanoparticles in the biomedical field as nanosensor for the detection of specific analytes. Hence, a sensor is by definition a device that reacts to a biological, chemical, or physical pattern and interprets its reaction into a signal modification [6]. Actually, to determine a perfect recognition of the irregular expression of a certain illness, the nanosensor should not interfere with other similar compounds to the essential analyte. Thus, conventional sensors such as microelectrode or fiber optical sensors suffer from their low selectivity due to their large area and size that trigger physical noise [7]. Based on these facts, it was necessary to develop nanosensors that are cheap, easy to manipulate along with high selectivity towards specific analytes. Thus, silica nanomaterials are being widely used and investigated as nanosensors for the estimation of biological molecules, heavy metals, etc. For example, Othman et al. have arisen the use of silica nanoparticles in the formation of liposomal curcumin for the selective estimation of ATP molecule [8]. Moreover, a recent study handled by El-Kurdi et al. has proven the efficiency of silica nanoparticles coated by chitosan oligosaccharides for the detection of mercury ions [9].

In recent years, there has been an increase in the presence of Ag⁺ in the environment because of human activities.

✉ Digambara Patra
dp03@aub.edu.lb

¹ Department of Chemistry, American University of Beirut, Beirut, Lebanon



Scheme 1: Schematic representation of the SiO₂ NPs synthesis

This increase is found in drinking water and food chains consumed by humans and leads to an accumulation of this metal ion in the human body that causes cell toxicity and organ failure [10, 11].

Generally, silver is found either in air, water, soil, and/or food. In fact, the US Environmental Protection Agency (EPA) has listed silver as a Group D carcinogen and has recognized an oral reference dose at a daily intake limit of 0.005 mg/kg. According to EPA, “minimal dietary exposure may result from the use of silver in human drinking water system”. Consequently, it was necessary to find suitable methods that help in estimating silver ions concentration [12]. The common methods used to detect silver ions are atomic absorption spectrometry [13, 14], inductively coupled plasma-mass spectrometry (ICP-MS) [15, 16], and ionic selective electrode [17]. However, these techniques present several limitations. On the first hand, they are extremely expensive, and on the other hand, they require complicated sample preparations and demand experienced engineers for their repairs [18, 19]. Henceforward, it was the need to find simple, fast, with low cost technique for the detection of Ag⁺ ions. Thus, resonance Rayleigh scattering (RRS) was one of the most easiest techniques to be applied in sensing application. In fact, RRS is a distinctive elastic scattering formed when the wavelength of Rayleigh scattering (RS) is located at/or close to the molecular absorption band. RRS means that for an excited sample, the transmission, reflection and coherent emission exist in other directions [20].

Henceforth in this study, we optimized the reaction’s parameters as a first step, by studying the effect of the silica precursor on the size of the nanoparticles, and the effect of the concentration of NaOH added. The most stable NPs

were then taken and used for the detection of Ag⁺ using RRS technique.

Materials and Methods

Materials

Colloidal silica suspension (size = 20 nm) was purchased from Sigma-Aldrich. Pure ethanol and sodium hydroxide (NaOH), tetraethyl orthosilicate (TEOS), silica gel, and (3-aminopropyl) triethoxysilane were obtained from Sigma-Aldrich. Silver nitrate (AgNO₃) was obtained from Sigma-Aldrich. Mercury (II) nitrate monohydrate (Hg(NO₃)₂·H₂O), nickel (II) nitrate hexahydrate (Ni(NO₃)₂·6H₂O), lead (II) nitrate (Pb(NO₃)₂), aluminum nitrate nonahydrate (Al(NO₃)₃·9H₂O), sodium nitrate (NaNO₃), zinc nitrate hexahydrate (Zn(NO₃)₂·6H₂O), and potassium nitrate (KNO₃) were acquired from Acros. All chemicals were used as received without any further purifications, and dissolved in double distilled water.

Synthesis of Silica Dioxide Nanoparticles

The preparation of colloidal silica nanoparticles was carried out based on Rao et al. [21], with some modifications (see Scheme 1). Initially, 5 mL of double distilled water (DDW) were mixed with 5 mL of pure ethanol and sonicated for 20 min. Later on, 1 mL of colloidal silica was added drop wise to the solvent mixture with continuous sonication. Afterward, 2 mL of NaOH (C = 1 mol/L) were added and the mixture was stirred for 1 h at 400 rpm to ensure the formation of

a turbid white precipitate. This precipitate was then isolated from the solution by centrifugation at 4000 rpm for 15 min. In order to eliminate the EtOH traces, the precipitate was washed twice with DDW and centrifuged again at 4000 rpm for 15 min. Finally, the solution was kept under freeze dryer for 24 h in order to get a white dehydrated powder.

Optimization of the Reaction Parameters

The size, shape, etc., depend intensely on the reaction parameters. For this reason, the reaction parameters were optimized in order to prepare the most stable, and the smallest SiO₂ NPs. For this purpose, different silica precursors were used, and NaOH concentration was varied.

Effect of Silica Precursor

In this step, 4 different solutions were prepared, each containing different silica precursor. The different silica precursors used were tetraethyl orthosilicate (TEOS, $V=1$ mL), (3-aminopropyl) triethoxysilane (APTMS, $V=1$ mL), silica gel ($m=1.12$ g), and colloidal silica ($V=1$ mL). After that, the synthesis was completed as described in the “[Synthesis of Silica Dioxide Nanoparticles](#)” section.

Effect of Sodium Hydroxide's Concentration

After choosing the adequate silica precursor, the effect of NaOH's concentration was expanded. For this reason, a stock solution of NaOH ($C=6$ M) was prepared by dissolving 2.4 g of NaOH in 10 mL of double distilled water. From this stock solution, different concentrations of NaOH were added to the mixture of DDW, EtOH, and silica precursor. The NaOH concentration used was equal to 50 mM, 100 mM, 500 mM, 1 M, and 3 M. Similarly, the synthesis was continued as described in the “[Synthesis of Silica Dioxide Nanoparticles](#)” section.

Characterization and Spectroscopic Analysis

For measuring resonance Rayleigh scattering spectrum (RRS), synchronous fluorescence scan mode was used at a wavelength interval ($\Delta\lambda=0$ nm). Synchronous fluorescence scan was measured using Jobin–Yvon-Horiba Fluorolog III fluorometer and the FluorEssence program. The excitation source was a 100 W Xenon lamp, and the detector used was R-928 operating at a voltage of 950 V by keeping the excitation and emission slits width at 0 nm.

The X-ray diffraction (XRD) data were recorded using a Bruker d8 discover X-ray diffractometer equipped with Cu-K α radiation ($\lambda=1.5405^\circ$). The monochromator used was Johansson type. The step size was 0.02 s and the scan rate was 20 s per step.

Furthermore, the thermogravimetric analysis (TGA) measurements were done using a Netzsch TGA 209 in the temperature range 30 to 1000 °C with an increment of 10/min in a N₂ atmosphere. Scanning electron microscopy (SEM) analysis was done using Tescan, Vega 3 LMU with Oxford EDX detector (Inca XmaW20). In short, SiO₂ NPs powder were deposited on an aluminum stub and coated with carbon conductive adhesive tape.

Finally, the zeta potential was measured using the dynamic light scattering machine (Manufacturer: Particulate systems, Model: NanoPlus HD Zeta Potential/Nano Particle analyzer).

Sample Preparation for Silver Nitrate Detection

The detection of aqueous silver ions was performed using SiO₂ NPs solutions at room temperature. In summary, 300 μ M stock solution of silver ions was prepared by dissolving 0.85 mg of AgNO₃ in 10 mL of double distilled water. To arrange several known concentrations in the range of 0 to 300 μ M, a known volume of stock solution of silver ion was pipetted and added to 0.1 mg/mL of SiO₂ NPs aqueous solution. The detection of Ag⁺ ions was done using resonance Rayleigh scattering. To adjust the final concentration, a complementary volume of double distilled water was added to make a total volume of 3 mL.

Results and Discussion

Optimization of the Reaction Parameters

The preparation of SiO₂ NPs was carried out through one simple synthesis route by sol–gel process. In this procedure, different shapes and sizes could be obtained when varying the reaction parameters. The effect of silica precursor, and NaOH's concentration was developed and the obtained SiO₂ NPs were compared and characterized through XRD, TGA, and SEM.

Effect of Silica Precursor

Briefly, 5 mL of double distilled water were mixed with 5 mL of ethanol and left in a sonication bath for 20 min. After that, each 1 mL of the 4 silica precursors was added (TEOS, APTMS, silica gel, and colloidal silica) separately to the different samples followed by the addition of 2 mL of NaOH ($C=1$ M). After 1 h, when using APTMS and silica gel as precursors, no white precipitate was formed. However, in the presence of colloidal silica and TEOS, a white turbid suspension appeared. Meaning that, the reaction occurred only when colloidal silica and TEOS were used. After the reaction was done, the precipitate was freeze dried and characterized through XRD, TGA, and SEM.

According to Nallathambi et al. [22], the XRD diffraction pattern of silica nanoparticles powder usually shows a broad peak at $2\theta = 22^\circ$. Similar results were obtained for both SiO_2 NPs prepared using TEOS and colloidal silica, confirming the amorphous nature of silica nanoparticles (see Fig. S1A, see Supporting Information, SI), although a minor shift in the diffraction angle was observed for TEOS where $2\theta = 25^\circ$. This difference is due to the fact that TEOS has a long carbon chain (C_8H_{20}) which is absent in colloidal silica [23]. Furthermore, thermogravimetric analysis TGA was measured in order to check the thermal stability of the produced NPs. As shown in Fig. S1B (see SI), the SiO_2 NPs were found to be highly stable with the increase of the temperature from 30 to 1000 °C. In fact, the TGA analysis showed a weight loss around $\sim 100^\circ\text{C}$ for both colloidal silica and TEOS. Initially, this weight loss is attributed to the loss of water and ethanol. Additionally, the TGA results indicate that a mass loss of $\sim 7\%$ happened when colloidal silica was used and of $\sim 14\%$ when TEOS was used. Similarly, the highest % mass loss of TEOS is mainly attributed to the presence of long carbon chain in TEOS structure.

Finally, scanning electron microscopy was carried out to compare the size of the particles obtained when varying the silica precursor. As shown in Fig. 1A, when TEOS was used large spheres were obtained in the range of 300–500 nm. However, a huge difference was obtained when using

colloidal silica, where the size has decreased dramatically to 40–50 nm (see Fig. 1B). To sum up, the silica precursor that will be used throughout the experiment is colloidal silica since the nanoparticles obtained using this precursor were the most stable with small size.

Effect of NaOH Concentration

In fact, the use of NaOH in this experiment is critical since silicon dioxide nanoparticles are being produced. For this purpose, the concentration of NaOH was varied from 50 mM to 3 M and the formed NPs were also compared through XRD, TGA, and SEM techniques. Henceforth, for a concentration equal to 50 mM, the reaction was almost incomplete, since after 1 h, a pale turbidity was obtained, resulting in few nanograms of the powder formed. However, when the concentration of NaOH increased, a white precipitate appeared, verifying the total formation of SiO_2 NPs. Hence, the obtained NPs were characterized principally via XRD analysis. In fact, no change was found in the X-ray diffractogram of the different SiO_2 NPs prepared using different NaOH concentration. However, this was expected since the NaOH concentration has no direct effect on the crystallinity degree of the nanoparticles. Hence a broad peak was shown at $2\theta = 22^\circ$ meaning that no alterations were done on the amorphousness structure of these NPs (see Fig. 2A). Moreover, as shown in Fig. 2B

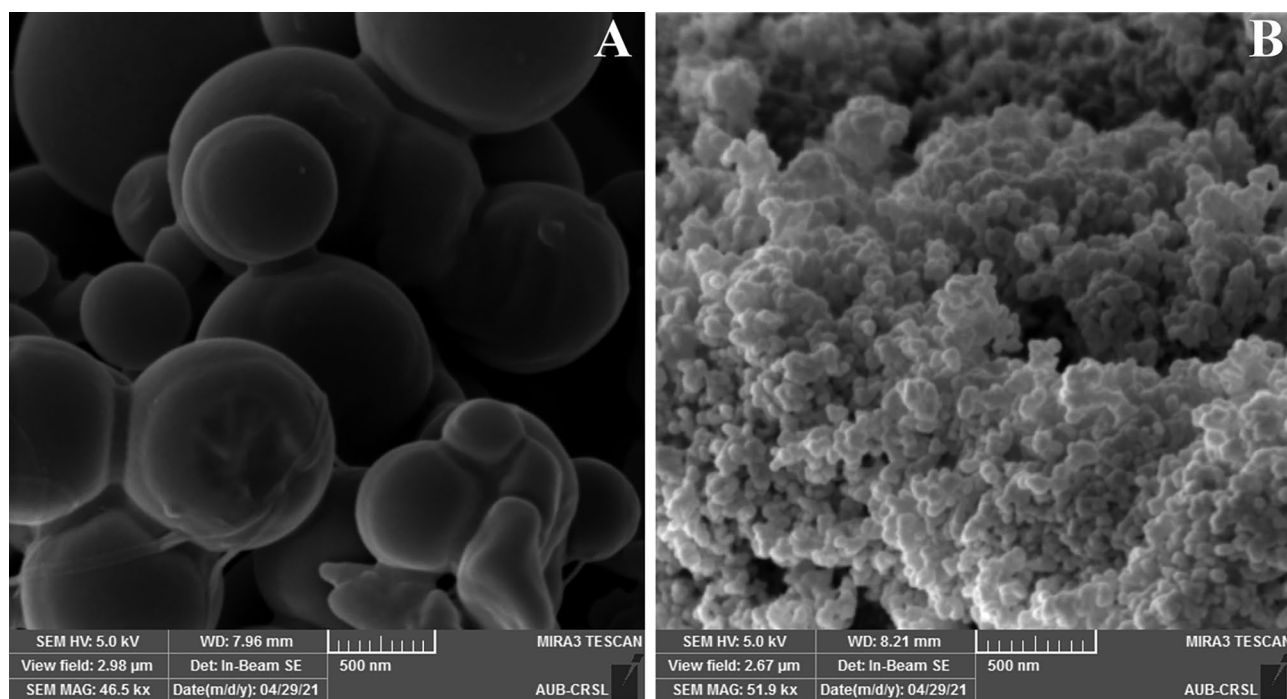


Fig. 1 SEM image of SiO_2 NPs using **A** TEOS and **B** using colloidal silica

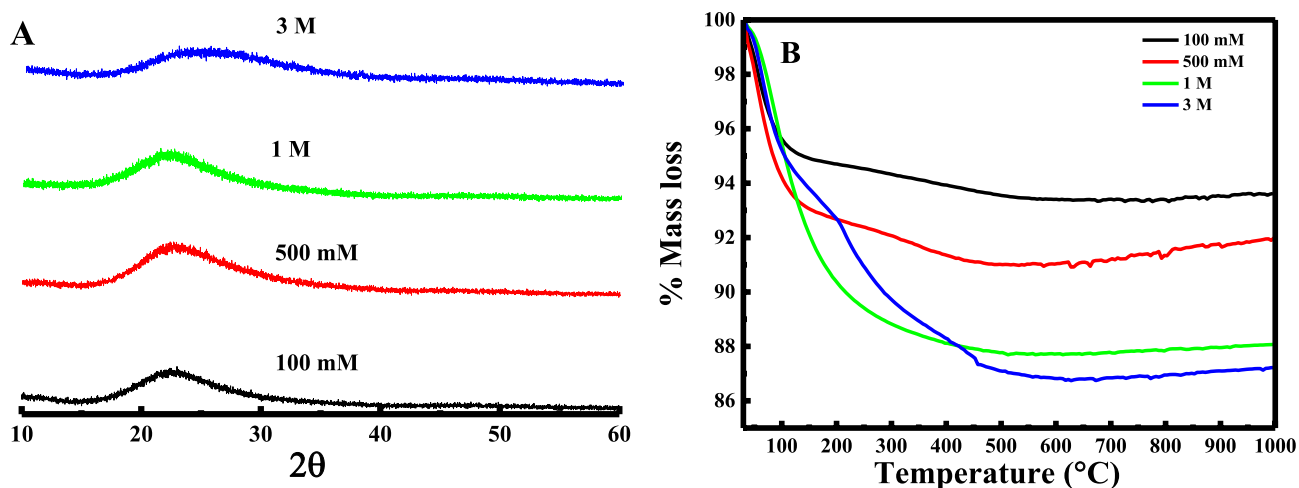


Fig. 2 **A** PXR D pattern of SiO₂ NPs and **B** thermogravimetric analysis TGA prepared with different NaOH concentrations

from the TGA analysis, a minimal weight loss occurred around ~100 °C, attributed to the loss of H₂O and EtOH, yet when using 3 M NaOH a mass loss of ~14% happened; thus, only ~4% weight loss occurred when 100 mM of NaOH were used. Consequently, the difference in the mass loss percentage is due to the presence of excess concentration of NaOH.

Finally, SEM was carried out to compare the size of the NPs formed. As shown in Fig. 3A–D, when the concentration of NaOH increased, the size of the NPs increased as well. For instance, the size of the formed SiO₂ NPs increased from 20–50 nm to 200 nm, when the NaOH concentration increased from 100 mM to 3 M. These results were expected, where the excess of NaOH improve the formation of aggregate in the solution. Hence, the concentration of NaOH that was chosen to use throughout the other experiments was 100 mM since the most stable and smallest NPs in size formed were when using this concentration.

Detection of Silver Cations

In fact, Laurent et al. have proven that the use of different nanomaterials in various biomedical applications necessitate that the NPs have great magnetization value, a size less than 100 nm and a narrow particle size distribution [24]. Consequently, Santra et al. agreed that the interaction of contaminants with NPs is particularly dependent on the NPs characteristics, essentially their size [25]. Therefore, based on Rogozea et al. work, the high surface area of NPs obtained, due to their very small size will extremely facilitate the efficient reaction between the NPs and the analytes in different reaction [26]. Based on these evidences, the SiO₂ NPs prepared using 1 mL of colloidal silica in the presence of 100 mM NaOH are used as nanoprobes for the detection of silver ions.

Sensing Ability

The application of the resonance Rayleigh scattering (RRS) signal was applied for the examination of the sensitivity of the SiO₂ NPs sensing probe. For this aim, different concentrations of silver ion in the range of 5 to 300 μM were added to the SiO₂ NPs solution. Figure 4 shows the RRS spectra of SiO₂ NPs after adding different concentration of silver ions. The RRS peak of SiO₂ NPs presented at $\lambda = 398$ nm has been proportionally improved with the increase in silver ion concentrations. This increase in the RRS intensity is due to the adsorption of Ag⁺ ions onto the mesoporous surface of the SiO₂ NPs.

Furthermore, the RRS intensities at $\lambda = 398$ nm have been plotted versus the concentration of silver ions in the range 5–300 μM. Figure 5 shows a linear increase in the RRS intensity within the increase of the concentration, within a linear equation $y = 339,050.51x + 8.63 \times 10^6$ and a regression coefficient R^2 equal to 0.9916. Interestingly, the limit of detection (LOD) and quantification (LOQ) were found to be 130 nM and 405 nM respectively, referring to $k\sigma/s$ criteria, where σ is the standard deviation of y-intercepts of regression lines, k is the constant ($k = 3.3$ for the LOD and $k = 10$ for LOQ), and s is the slope of the calibration curve. The obtained results reveal that our RRS method leads to a comparable linear range and limit of detection to those of previously reported methods (see Table 1). It was found that the present method works in higher concentration range and has a higher linear dynamic range.

Mechanism of the Proposed Nanosensor

As mentioned earlier, the increase in the RRS intensity was attributed to the adsorption of positively charged Ag⁺ to the negatively charged mesoporous SiO₂ NPs nanoprobes.

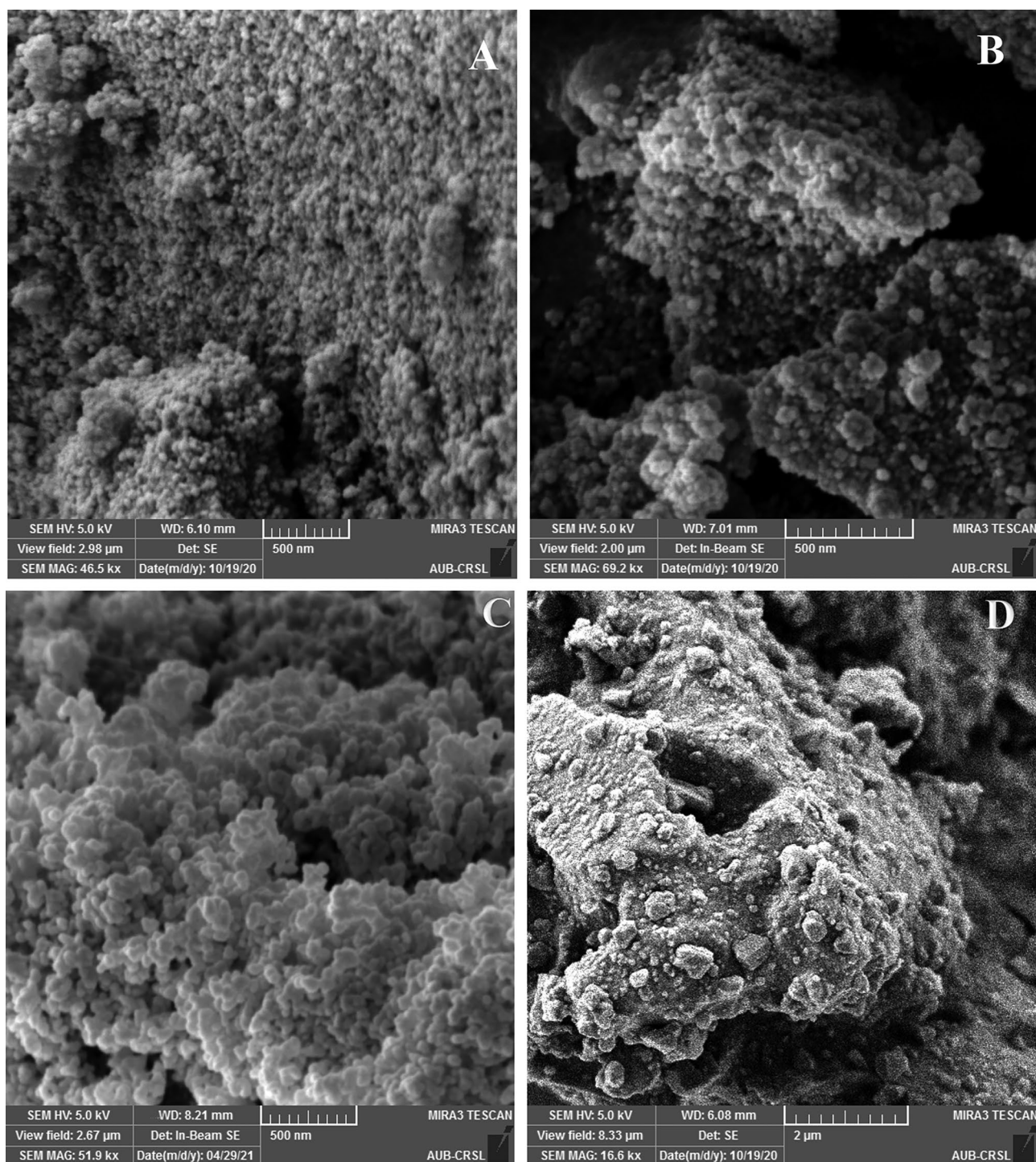


Fig. 3 SEM images of SiO_2 NPs prepared with different concentrations of NaOH **A** 100 mM; **B** 500 mM; **C** 1 M, and **D** 3 M

This adsorption is commonly due to the electrostatic interaction between two opposite charged species. According to Eftekhari et al. [32], silica nanoparticles are negatively charged in a pH range of 2 to 14. This confirms the electrostatic interaction happening between the negatively

charged SiO_2 NPs and the Ag^+ ions, positively charged. This statement was verified when measuring the surface charge of the nanosensor, and the mixture using zeta potential analysis. In fact, the surface charge of the SiO_2 NPs was equal to -19.08 mV. The charge of the surface increases

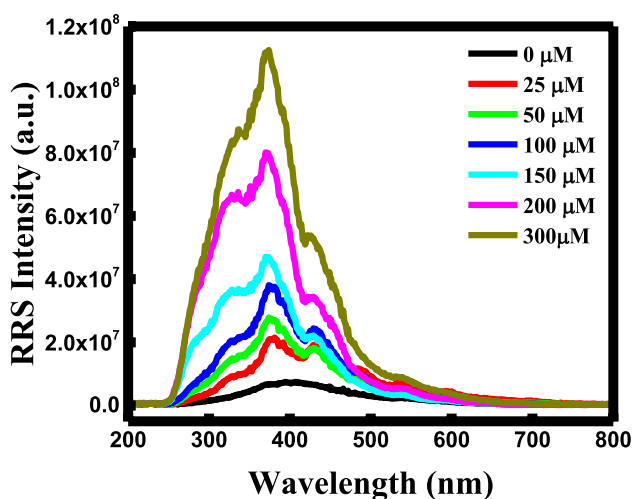


Fig. 4 Resonance Rayleigh scattering spectrum of SiO₂ NPs in the presence of silver cations in the range of 5–300 μM

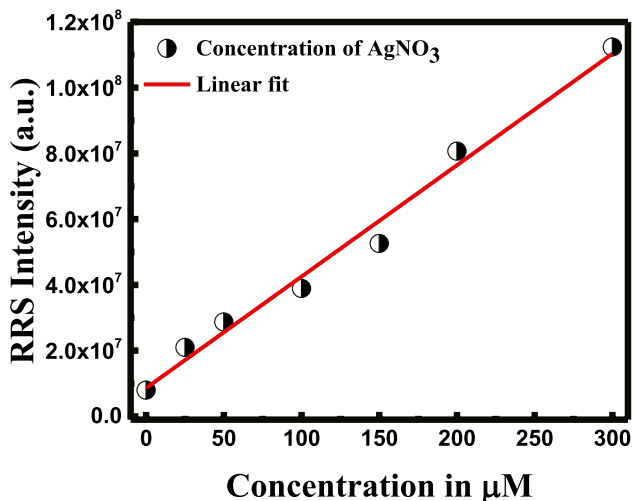


Fig. 5 Linear fit of the proposed method in the range of 5–300 μM

to -4.28 mV upon the addition of silver ions. This change in the surface charge reveals the presence of more positive species which are related to silver ions adsorbed on the surface of SiO₂ NPs (see Fig. S2. SI).

Interferences in Silver Detection

It is of great importance to study the selectivity of the developed nanoprobe, particularly in real sample applications. Accordingly, different control experiments were done using different $M^{x+} NO_3^-$ such as, Cu²⁺, Hg²⁺, Ni²⁺, Pb²⁺, Al³⁺, Na⁺, Zn²⁺, and K⁺ ($C = 300 \mu M$), in order to test the selectivity of our sensing approach for Ag⁺ detection. The ratio of the RRS intensity in the presence of the different analytes, to the RRS intensity in the absence of these analytes (I/I_0) was measured and shown in Fig. 6A. I/I_0 ratio showed a same value of ~ 2 for Ni²⁺, Pb²⁺, Zn²⁺, and K⁺. This value decreased and reached ~ 1 for Hg²⁺ and Na⁺ and a value of ~ 0.5 for Al³⁺. However, for Ag⁺, I/I_0 ratio was ~ 28 . Thus, it is clear that the synthesized silicon dioxide nanoparticles were extremely selective towards Ag⁺ ions. To understand the selective detection towards silver ions, the topological surface area of each metal ion was found and compared (see Table 2). In fact, mercury (II) nitrate, nickel (II) nitrate, lead (II) nitrate, aluminum nitrate, and zinc nitrate hexahydrate possess high topological polar surface area. Thus, silver nitrate, sodium nitrate, and potassium nitrate have equal surface area, yet only silver ions can interact with SiO₂ NPs since silver is considered as a transition metal and it exhibits the highest electrical conductivity, increasing thereby the electrostatic interaction within the SiO₂ NPs.

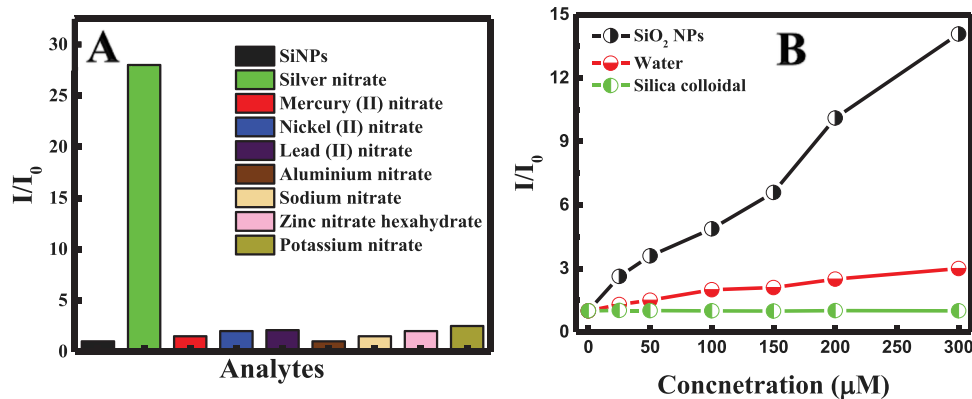
Selectivity Towards the Nanoprobe

The selectivity of the synthesized colloidal silica nanoparticles was investigated in the absence of SiO₂ NPs nanoprobe,

Table 1 Different techniques used for the detection of silver ion

Sensing technique	Range	LOD	Interference	Reference
Fluorescence biosensor based on C–Ag + -C structure and exonuclease III-assisted dual-recycling amplification	5–1500 pmol/L	2 pmol/L	Na ⁺ , Hg ²⁺ , Pd ²⁺ , Cd ²⁺ , Cu ²⁺ , Zn ²⁺ , Ni ²⁺ , Al ³⁺ , Fe ³⁺	[27]
Colorimetric detection	10 ⁻² –10 ⁴ nM	80 pM	NH ₄ ⁺ , Na ⁺ , K ⁺ , Li ⁺ , Ba ²⁺ , Ca ²⁺ , Cd ²⁺ , Co ²⁺ , Cu ²⁺ , Fe ²⁺ , Mg ²⁺ , Mn ²⁺ , Ni ²⁺ , Pb ²⁺ , Zn ²⁺ , Al ³⁺ , Cr ³⁺ , Fe ³⁺ , Cu ⁺ , Pd ²⁺ , Hg ²⁺	[28]
Fluorescent detection with organic nano-aggregates	----	11 ppb	Na ⁺ , K ⁺ , Cr ³⁺ , Mn ²⁺ , Fe ²⁺ , Fe ³⁺ , Hg ²⁺ , Co ²⁺ , Ni ²⁺ , Cu ²⁺ , Zn ²⁺ , and Pb ²⁺	[29]
Detection of silver ions using DNA based nanoporous micro-resonator	10 nM–1 pM	1 nM	Na ⁺ , Li ⁺ , Ca ²⁺ , Mg ²⁺ , Zn ²⁺ , and Fe ²⁺	[30]
Colorimetric detection using gold nanoparticles in the presence of ascorbic acid	2–28 μM	0.85 μM	Al ³⁺ , Mg ²⁺ , Mn ²⁺ , Ni ²⁺ , Ca ²⁺ , Zn ²⁺ , Na ⁺ , Co ²⁺ , Cu ²⁺ , Cd ²⁺ , Fe ²⁺ , Fe ³⁺ , Pb ²⁺ , Hg ²⁺ , and K ⁺	[31]
RRS using silica nanoparticles	5–300 μM	130 nM	Cu ²⁺ , Hg ²⁺ , Ni ²⁺ , Pb ²⁺ , Al ³⁺ , Na ⁺ , Zn ²⁺ , and K ⁺	Our work

Fig. 6 A I/I_0 of SiO_2 NPs in the presence of $300 \mu\text{M}$ for different cations; B I/I_0 of silver ions detection in the presence of SiO_2 NPs, water, and silica colloidal



and by replacing the prepared nanoparticles with the silica precursor (colloidal silica suspension). As shown in Fig. 6B, no detection was observed nor in the presence of colloidal silica suspension and nor when dissolving in water. Hence, the synthesized colloidal silica nanoparticles SiO_2 NPs were proved to act as an efficient nanoprobe for the detection of silver ions.

Determination of Silver Ions in Real Samples

The proposed silicon dioxide nanoparticles were used to determine the concentration of silver ions in water samples. The water samples were obtained from two different drinking water suppliers. The original drinking water samples showed no detectable silver ions. For this purpose, each sample had been spiked with known concentration of silver ions in order to get the recovery of the experiment. As shown in Table 3, the recovery percentages of the spiked samples were found to be relatively high, in the range 98.4–100.4%.

Photostability of the Proposed Nanosensor

The photo-stability of SiO_2 NPs in the presence and absence of Ag^+ ions is illustrated in Fig. S3 (see, SI). It was found

Table 2 Topological surface area of different metal ions

Metal	Topological surface area
Silver nitrate	62.9 \AA^2
Mercury (II) nitrate	126 \AA^2
Nickel (II) nitrate	126 \AA^2
Lead (II) nitrate	126 \AA^2
Aluminium nitrate	189 \AA^2
Sodium nitrate	62.9 \AA^2
Zinc nitrate hexahydrate	126 \AA^2
Potassium nitrate	62.9 \AA^2

Table 3 Percentage recovery of the proposed method

	Theoretical concentration (μM)	Experimental concentration (μM)	Recovery (%)
Unknown 1	5	4.98	99.6
Unknown 2	75	73.8	98.4
Unknown 3	250	251.01	100.4

that in the presence and absence of Ag^+ , the I/I_0 ratio was not altered within 1 h. These results indicate that the current sensor is relatively stable during measurement within time.

Conclusion

In conclusion, SiO_2 NPs were synthesized through a simple method by sol–gel process. It was found that the most efficient NPs were formed when 1 mL of colloidal silica (0.66 M) was used in the presence of 2 mL of NaOH with a concentration of 100 mM. The produced nanoparticles have shown high thermal stability, and formed in a spherical shape between 20 and 50 nm. These properties have improved the use of SiO_2 NPs as a nanoprobe for the detection of silver ions. In addition, the obtained NPs showed a highly effective method for the detection of Ag^+ ions using RRS technique. This method has shown a selective detection of silver ions, compared to other analytical methods such as chromatography, electrochemical techniques, and spectrophotometric absorption. The use of RRS technique decreases the limitations of the analytical methods such as source of errors using electrodes, same retention time for different analytes in HPLC, GC, or AA. Hence, it offers the detection of silver ions in a wider range from 5–300, with low LOD value equal to 130 nM and a LOQ of 405 nM. Finally, the recovery of the methods was relatively high between 98.4 and 100.4%.

Supplementary Information The online version contains supplementary material available at <https://doi.org/10.1007/s11468-022-01627-6>.

Acknowledgements The authors greatly acknowledged Kamal A. Shair Central Research Laboratory (KAS CRSL) facilities for carrying out this work.

Author Contribution Junstine Dagher contributed in methodology, formal analysis, investigation, experiment, validation, writing—original draft preparation; Riham El Kurdi contributed in formal analysis, experiment, analysis, writing—reviewing and editing; and Digambara Patra contributed in conceptualization, supervision, resources, project administration, writing—reviewing and editing.

Funding This work is funded by the American University of Beirut, Lebanon through URB.

Declarations

Ethics Approval Not applicable.

Consent to Participate Not applicable.

Consent for Publication Not applicable.

Competing Interests The authors declare no competing interests.

References

- Vert M, Doi Y, Hellwich KH, Hess M, Hodge P, Kubisa P, Rinaudo M, Schué FO (2012) Terminology for biorelated polymers and applications (IUPAC Recommendations 2012). *Pure Appl Chem* 84(2):377–410
- Abi RI, Padavettan V (2012) Synthesis of silica nanoparticles by sol-gel: size-dependent properties, surface modification, and applications in silica-polymer nanocomposites—a review. *J Nanomater* 2012:1–15
- Kakoty V, Sarathlal KC, Pandey M, Dubey SK, Kesharwani P, Taliyan R (2021) Biological toxicity of nanoparticles. *Nanoparticle Therapeutics*
- Park SK, Kim KD, Kim HT (2002) Preparation of silica nanoparticles: determination of the optimal synthesis conditions for small and uniform particles. *Colloids Surf A* 197(1–3):7–17
- Roy I, Ohulchanskyy TY, Pudavar HE, Bergey EJ, Oseroff AR, Morgan J, Dougherty TJ, Prasad PN (2003) Ceramic-based nanoparticles entrapping water-insoluble photosensitizing anticancer drugs: a novel drug-carrier system for photodynamic therapy. *J Am Chem Soc* 2003(125):7860–7865
- van Zee RD, Pomrenke GS (2009) Nanotechnology-enabled sensing. *Rep Natl Nanotechnol Initiat Work* [Online]
- Cullum BM, Vo-dinh T (1938) The development of optical biosensors for biological measurement. *BMJ* 1(4017):20–21
- Othman A, El-Kurdi R, Patra D (2021) Outstanding enhancement of curcumin fluorescence in PDAA and silica nanoparticles coated DMPC liposomes based nanocapsules: application for selective estimation of ATP. *ChemistrySelect* 6(25):6324–6332
- El Kurdi R, Chebl M, Sillanpää M, El-Rassy H, Patra D (2021) Chitosan oligosaccharide/silica nanoparticles hybrid porous gel for mercury adsorption and detection. *Mater Today Commun* 28:102707
- Arora S, Lidor A, Abularrage CJ, Weiswasser JM, Nylen E, Kellcutt D, Sidawy AN (2006) Thiamine (vitamin B1) improves endothelium-dependent vasodilatation in the presence of hyperglycemia. *Ann Vasc Surg* 20(5):653–658
- Wygładacz K, Radu A, Xu C, Qin Y, Bakker E (2005) Fiber-optic microsensor array based on fluorescent bulk optode microspheres for the trace analysis of silver ions. *Anal Chem* 77(15):4706–4712
- United States Environmental Protection Agency (1993) Silver. R.E.D. Facts
- López-López JA, Jönsson JA, García-Vargas M, Moreno C (2014) Simple hollow fiber liquid membrane based pre-concentration of silver for atomic absorption spectrometry. *Anal Methods* 6(5):1462–1467
- López-López JA, Herce-Sesa B, Moreno C (2016) Solvent bar micro-extraction with graphite atomic absorption spectrometry for the determination of silver in ocean water. *Talanta* 159:117–121
- Balcaen L, Bolea-Fernandez E, Resano M, Vanhaecke F (2015) Inductively coupled plasma–Tandem mass spectrometry (ICP-MS/MS): a powerful and universal tool for the interference-free determination of (ultra)trace elements—a tutorial review. *Anal Chim Acta* 894:7–19
- Ramos K, Ramos L, Gómez-Gómez MM (2017) Simultaneous characterisation of silver nanoparticles and determination of dissolved silver in chicken meat subjected to in vitro human gastrointestinal digestion using single particle inductively coupled plasma mass spectrometry. *Food Chem* 221:822–828
- Lai C-Z, Fierke MA, da Costa RC, Gladysz JA, Stein A, Bühlmann P (2010) Highly selective detection of silver in the low ppt range with ion-selective electrodes based on ionophore-doped fluorinated membranes. *Anal Chem* 82(18):7634–7640
- Kim HN, Ren WX, Kim JS, Yoon J (2012) Fluorescent and colorimetric sensors for detection of lead, cadmium, and mercury ions. *Chem Soc Rev* 41(8):3210–3244
- Quang DT, Kim JS (2010) Fluoro- and chromogenic chemodosimeters for heavy metal ion detection in solution and biospecimens. *Chem Rev* 110(10):6280–6301
- El-Kurdi R, Patra D (2019) Gold and silver nanoparticles in resonance Rayleigh scattering techniques for chemical sensing and biosensing: a review. *Microchim Acta* 186:667
- Rao K, El-Hami K, Kodaki T, Matsushige K, Makino K (2005) A novel method for synthesis of silica nanoparticles. *J Colloid Interface Sci* 289:125–131
- Nallathambi G, Ramachandran T, Rajendran V, Palanivelu R (2011) Effect of silica nanoparticles and BTCA on physical properties of cotton fabrics. *Mater Res* 14(4):552–559
- Kim KD, Kim HT (2002) Formation of silica nanoparticles by hydrolysis of TEOS using a mixed semi-batch/batch method. *J Sol-Gel Sci Technol* 25:183–189
- Laurent S, Forge D, Port M, Roch A, Robic C, Vander Elst L, Muller RN (2008) Magnetic iron oxide nanoparticles: synthesis, stabilization, vectorization, physicochemical characterizations, and biological applications. *Chem Rev* 108:2064–2110
- Santra S, Zhang P, Wang K, Tapeç R, Tan W (2001) Conjugation of biomolecules with luminophore-doped silica nanoparticles for photostable biomarkers. *Anal Chem* 73:4988–4993
- Rogozea EA, Petcu AR, Olteanu NL, Lazar CA, Cadar D, Mihaly M (2017) Tandem adsorption-photodegradation activity induced by light on NiO-ZnO p-n couple modified silica nanomaterials. *Mater Sci Semicond Process* 57:1–11
- Li Y, Yan J, Xu Z (2019) A sensitive fluorescence biosensor for silver ions (Ag⁺) detection based on C-Ag⁺-C structure and exonuclease III-assisted dual-recycling amplification. *J Anal Methods Chem* 2019
- Gao Z, Liu GG, Ye H, Rauschendorfer R, Tang D, Xia X (2017) Facile colorimetric detection of silver ions with picomolar sensitivity. *Anal Chem* 89:3622–3629
- Hatai J, Pal S, Bandyopadhyay S (2012) Fluorescent detection of silver ions in water with organic nano-aggregates. *RSC Adv* 2:10941–10947

30. Jang K, You J, Park C, Na S (2017) Highly sensitive detection of silver ions using a silver-specific DNA based nano-porous micro-resonator. *New J Chem* 41(4):1840–1845
31. Selva Sharma A, SasiKumar T, Ilanchelian M (2018) A rapid and sensitive colorimetric sensor for detection of silver ions based on the non-aggregation of gold nanoparticles in the presence of ascorbic acid. *J Cluster Sci* 29(4):655–662
32. Eftekhari M, Schwarzenberger K, Javadi A, Eckert K (2020) The influence of negatively charged silica nanoparticles on the surface properties of anionic surfactants: electrostatic repulsion or the effect of ionic strength?. *Phys Chem Chem Phys* 22:2238–2248

Publisher's Note Springer Nature remains neutral with regard to jurisdictional claims in published maps and institutional affiliations.